Fusion dynamics of mass-asymmetric reactions using Skyrme based nuclear potentials

A Dissertation

Submitted in Partial Fulfillment of the Requirement for the Award of Degree of

Master of Science

In

Physics

Submitted By:

Amritpal

Roll No. 301904001

Under the supervision of

Dr. Manoj K. Sharma

Professor

TIET Patiala

SCHOOL OF PHYSICS AND MATERIALS SCIENCE

THAPAR INSTITUTE OF ENGINEERING AND TECHNOLOGY, PATIALA

PUNJAB-147004

Dedicated to my Family,

and Friends.

Declaration

I hereby declare that the dissertation entitled **"Fusion dynamics of mass-asymmetric reactions using Skyrme based nuclear potentials"** is a genuine record of my work carried out as a requirement for the the award of the degree of **Master of Science** at **Thapar Institute of Engineering and Technology, Patiala** under the supervision of **Prof. Manoj K. Sharma**. The matter presented in this thesis has not been submitted by me, in parts or full, for the award of any other degree in any other university or institute.

29/07/2021
Dated:

Amritpal
(Amritpal)
301904001

It is certified that the above statement made by the student is correct to the best of my knowledge and belief.

29.7.2021
(Dr. Manoj K. Sharma)
Supervisor
Professor
TIET, Patiala

Acknowledgment

I would like to acknowledge and express my sincere gratitude for the opportunity and valuable guidance presented to me by **Prof. Manoj K. Sharma**, Professor, Thapar Institute of Engineering and Technology. It was his guidance and advice which made this work possible. I am thankful to him for giving me the flexibility and liberty to carry out this work. I am very grateful for his motivation, patience and immense knowledge.

I am highly obliged to **Prof. O. P. Pandey**, Head of Department, School of Physics and Materials Science, for his support and facilities provided. I would also like to thank all the faculty members of the School of Physics and Materials science, who were always accessible and helpful.

The thesis would not have come to a successful completion without the help I received from **Ms. Shivani Jain**, Research Scholar, School of Physics and Materials science, TIET, Patiala. I am very thankful for all the help and assistance provided by her. At last, I wish to sincerely thank all of my friends and classmates, who encouraged me throughout the course of this work.

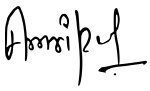

(Amritpal)

Contents

List of Tables

List of Figures

Abstract

The present work in this dissertation deals with a wide range of mass-asymmetric nuclear reactions (^{28,30}Si, ^{36}S, ^{40}Ca, ^{48}Ti+^{58}Ni, and ^{58}Ni+^{90}Zr, ^{92}Mo, ^{94}Zr and ^{100}Mo) using three-parameter Fermi (3pF) density function within the Skyrme Energy Density Formalism (SEDF). The results are analysed in terms of fusion barrier characteristics and fusion cross-sections, using different sets of Skyrme forces i.e. SkTI, MSL0, GSkI and SSk. The present work comprises of three chapters, a brief account of which is discussed below.

Chapter 1

Chapter 1 presents the general introduction of the nucleus-nucleus interactions and nuclear phenomena relevant for the study of nuclear fusion reactions or the formation of a compound nucleus. This chapter also contains the introductory idea of various Skyrme interactions and density functions used in the work.

Chapter 2

In Chapter 2, the description of SEDF is provided, which is utilized to define the short-range attractive nuclear part of the total interaction potential. Also, the expressions for two-parameter Fermi (2pF) and three-parameter Fermi (3pF) density functions are discussed. Finally, a brief description of Wong formula and extended ℓ-summed Wong model is given.

Chapter 3

Chapter 3 contains the calculations and outcomes of the work done. The calculations are carried out for the asymmetric nuclear partners using the Skyrme interactions SkTI, MSL0, GSkI and SSk within the framework of SEDF. The fusion cross-sections are calculated by using the Wong formula and extended ℓ-summed Wong model over a wide range of center of mass energies, $E_{c.m.}$. The relevant outcomes are discussed in context of fusion dynamics involving asymmetric colliding partners.

Chapter 1

Introduction

1.1 Introduction

According to the widely recognized theory, all the visible universe was originated from a single point, an event that is known as the Big Bang. All the elementary particles were created within a few micro-seconds of the Big Bang, and the universe was in a very hot and dense state known as the quark-gluon plasma. As the universe expanded and started cooling, the quarks and gluons became condense and gave birth to the baryons such as neutrons and protons. After a few minutes, the temperature cooled down and these light particles condensed together to form light mass nuclei such as deuterium and helium etc. It took a long time to understand the atomic structure where electrons and nuclei combine together to form an atom. Later on, extreme conditions of the supernovae sow the seeds of the heavy nuclei (having $Z \geq 2$ and $A \geq 4$) which have been extended upto superheavy regime in due course of time. The study of ion-ion interactions is very important in order to have a comprehend knowledge of the formation of new elements and related characteristics. Such investigations are of great interest and have imparted significant information on nuclear phenomena during last few decades. Though the nuclear reactions take place at a very small scale of fermi units, they have proved to be hugely relevant for various mankind applications.

The concept of Nuclear physics started with the discovery of radioactivity by the French scientist Henri Becquerel in 1896. Later on, the discoveries of the electron, given by J.J. Thomson [1] and existence of nucleus by Ernest Rutherford [2] described the internal picture of an atom, which was considered to be an elementary particle in the early days. Further James Chadwick in 1932 [3] showed that the neutral particles, known as neutrons reside in the nucleus alongside positively charged protons. So, a nucleus is considered to be composed of protons and neutrons, which impart almost similar nuclear impulse except for charge dependent Coulomb component in case of a proton. Ongoing

research in nuclear physics is mostly based on the study of nucleus-nucleus interactions under extreme conditions, and the extension of nuclear periodic table, where number of new elements and isotopes have been synthesised during last few decades.

1.2 Nuclear Reactions

All the stars, including the sun, are driven by the energy produced in the nuclear reactions. Therefore, the study of nuclear reactions is of great significance to study about the fundamental nature of the universe. To study the nuclear reactions in the laboratory, the two nuclei are made to collide with each other, where the incoming nucleus acts as a projectile and target nucleus is kept at rest in general. Among various types of nuclear reactions, the heavy-ion induced reactions (having nuclei with charge, $Z \geq 2$ and mass, $A \geq 4$) have gained a great interest in later times. The development of various heavy-ion accelerators and Radioactive Ion Beam (RIB) facilities have made it possible to perform these nuclear reactions at extreme conditions of mass, charge, energy and angular momentum etc. Based upon different reaction parameters and energies, the interaction between two nuclei occur, which leads to the production of different kind of product nuclei [4]. The reaction can either be a Compound Nucleus (CN) reaction or a non-Compound Nucleus (nCN) reaction. For instance, reactions such as elastic and inelastic scattering, deep inelastic collisions (DIC) and quasi-fission occur without forming a compound nucleus. However, the formation of a compound nucleus occurs in nuclear fusion reactions, when two nuclei get trapped in the deep pocket of potential after crossing the Coulomb barrier. Such exotic compound nucleus breaks into two comparable fragments giving nuclear fission reaction or it can de-excite by emitting the light particles (such as protons or neutrons) leaving behind a residual nucleus, the process is known as evaporation residue. The present work is constrained to study the nuclear fusion phenomena or formation of a compound nucleus. In most of the cases, the compound nucleus formed is highly exotic, and depends upon a number of different factors i.e., angular momentum, excitation energy, atomic mass and charge etc. The heavy-ion nuclear reactions can be classified into different domains depending upon the excitation energy [5]. In the low energy domain, the nuclear fusion reactions take place and the subsequent process such as fission, quasifission, evaporation residue, particle production, nuclear capture etc come

into picture.

1.3 Nuclear Fusion Reactions

In the low energy regime, the incident projectile possesses energy $\leq$ 15 MeV/nucleon and subsequently the surface interactions of projectile-target colliding pair takes place. The heavy-ion induced fusion reactions provide a deeper insight of the nuclear structure and associated properties. Also, the investigation of low energy heavy-ion induced fusion reactions helps us to study the heavy and super-heavy exotic nuclei, which lie near and around the beta stability valley. In view of this, studying the behaviour of different projectile-target combinations for the synthesis of variety of compound systems is one of the important and interesting topic.

Different projectile-target combinations are generally categorized as symmetric and asymmetric reactions. For symmetric reactions, the colliding nuclei are of same mass and charge numbers. Whereas, the projectile and target of different mass/charge numbers define the asymmetric reactions. Many authors have analyzed the role of symmetric and asymmetric kinds of heavy-ion induced reactions via the total interaction potential, and subsequently analyzed the fusion cross-sections, for example one may refer [6, 7, 8]. In other words, to study heavy-ion induced reactions, the total interaction potential is considered as an important aspect and is defined as a combination of long-range repulsive Coulomb, centrifugal potentials and short-range attractive nuclear potential. These contributing potentials lead to the formation of a deep pocket and a barrier height, which hinders the fusion of colliding nuclei. On the basis of this concept, the authors of Refs. [6, 7] have considered symmetric and asymmetric colliding nuclear partners and observed corresponding effects on fusion barrier, calculated by using different choice of proximity potentials. In [8], the authors have used different density functions (two- and three-parameter Fermi) within Skyrme Energy Density Formalism (discussed later) and studied the corresponding effects on barrier characteristics (barrier height (V_B), barrier position (R_B) and barrier curvature ($\hbar\omega_B$)) and fusion cross-sections. The two-parameter Fermi (2pF) density function used within SEDF approach is able to address the experimental data of symmetric reaction i.e. ^{58}Ni+^{58}Ni. However, the three-parameter Fermi (3pF) density function seems to be more appropriate for asymmetric reactions (^{8}B, ^{18}O

and ^{132}Sn+^{58}Ni) [8]. In the present work, we are considering 3pF density function within SEDF approach to study the fusion dynamics of asymmetric colliding nuclear partners in terms of barrier characteristics and fusion cross-sections. The considered choice of reactions are ^{58}Ni-based reactions, because they are known to show fusion hindrance at the below barrier energies, and it would be interesting to explore the significance of 3pF density function in addressing the experimental data for such reactions at sub-barrier energies. The compound nucleus formed from these reactions belong to the mass region $A_{CN} = 86 - 158$.

Owing to the study of a large number of heavy-ion induced fusion reactions, it has been observed that the fusion cross-sections show unusual behaviour in the sub-barrier region. In order to examine the fusion cross-sections in the below barrier region, it is very important to use an appropriate form of the nuclear potential (V_N) along with Coulomb potential (V_C) and the centrifugal potential (V_ℓ). The repulsive Coulomb potential which contributes to the long-range part of the total ion-ion interaction potential is well studied, however the attractive nuclear potential is still not fully understood. Therefore, many methods and ideas have been put forward in order to comprehend the true nature of nuclear potential and thereby the appropriate barrier characteristics (V_B, R_B and $\hbar\omega_B$).

1.4 Total Interaction Potential

The ion-ion interaction potential is used to find the possibility of fusion among mass-symmetric and mass-asymmetric colliding partners. Unlike the well-established repulsive potentials, different types of nuclear potentials i.e. square-well potential, exponential potential and Wood-Saxon potential have been used since the early days of Nuclear Physics. These potentials have been utilized in the study of nuclear fusion reactions. For instance, it has been observed that parameterization of a chosen Wigner potential as a constituent of total interaction potential seems unrealistic at times, and provides a rather poor fit to the fusion data, especially in the below barrier region. So, to address the below barrier fusion data i.e. in the region below the Coulomb barrier, an appropriate form of nuclear potential is required. Mainly, it is essential to learn about the ion-ion interaction potential, which helps us to study the fusion among same/different kind of nuclear partners. In view of this, many authors have worked out a detailed analysis

of mass-symmetric and mass-asymmetric nuclear reactions [7, 8]. The authors in Refs. [6, 7] have followed the proximity theorem and illustrated the role of different proximity potentials for above said reactions. Further, the study has been extended by using the Skyrme Energy Density Formalism (SEDF) [8, 9]. With the consideration of SEDF, one is able to understand the amalgamation of the densities of colliding nuclear partners. The use of Energy Density Formalism (EDF) has been really useful in calculating the properties of a nuclear system [10]. The microscopic background to build the EDF model is provided by the self-consistent Hartree-Fork model [11].

The Hartree-Fork (HF) model tries to reproduce most of the nuclear properties in the lowest order using the effective interactions. Before HF model, many attempts were made to clarify the relation between the nucleon-nucleon interaction force and the observed single particle properties. For example, in one approach, soft potentials were used in the framework of Goldstone expansion and in the second approach, short ranged repulsive potential was used in the framework of Brueckner-Goldstone expansion. In both the approaches, the fit to nuclear radii and binding energy turned out to be quite poor having unknown discrepancies. Which could be due to the ignorance of higher order terms or due to inadequacy of the soft potentials. Such discrepancies were removed within the HF model. The model for the effective interactions can execute the calculations in two different ways: the first is to derive the formalism in the lowest order and then parameterize the higher order corrections, and second is to parameterize the interaction as a whole.

In the earlier approach [12, 13, 14], the calculations are carried out within the framework of Brueckner's theory using the local density approximation for lower order terms and the higher order ones are added to account the discrepancies in the binding energy. Due to this approach, the effective force becomes density dependent and gives satisfactory results to the experimental data. Conversely, the approach of direct parameterization of effective force is rather less fundamental but has several benefits i.e., it provides better physical insight and is easy to extrapolate in case the of exotic nuclei. This approach might contain density-independent and density-dependent forces. Density-independent forces imply some complexities in describing the binding energies and nuclear radii, whereas density-dependent forces provide a fair explanation of these properties. Such kind of density-dependent forces are called as Skyrme interactions [15, 16].

In 1950s, Tony Hilton Royle Skyrme proposed a non-relativistic zero-range, density and momentum dependent nucleon-nucleon interaction known as Skyrme interaction/force. Due to its zero-range form, Skyrme interactions simplify the calculations and successfully describe the various nuclear properties. These forces depend on a limited number of parameters. By addressing properties of nuclei of different mass-region, many authors have developed different sets of Skyrme forces, which have variety of input parameters [17]-[20]. To study the heavy-ion induced reactions, the researchers have worked on different choices of Skyrme forces, which in turn influences the total interaction potential, especially barrier characteristics. That is to say, different Skyrme forces provide different barrier characteristics i.e., barrier height (V_B), position (R_B) and barrier curvature ($\hbar\omega_B$). Therefore, a number of Skyrme forces are used to describe the experimental results of different nuclear reactions. In the present work, we have used four sets of Skyrme forces i.e., SkTI, MSL0, GSkI and SSk. The SkTI force is characterized by an effective mass m^* (equal to the bare nucleon mass) and no spin gradient term having low spin-orbit dependence [21]. On the other hand, MSL0 is a modified Skyrme like interaction having an additional spin gradient term due to the tensor coupling with spin and gradient [22] and have higher spin-orbit dependence than SkTI. Skyrme interaction GSkI [23] also contains a spin gradient term but have much stronger spin-orbit dependence and mass asymmetry effects than MSL0. At last, the SSk force [23] is obtained using the same set of data as for GSkI but have comparatively low spin-orbit dependence. In literature, around 300 Skyrme interactions has been constructed and among them only a few forces are found to give satisfactory results for a large range of projectile and target combinations in the formation of a compound nucleus over a wide range of center of mass energies, $E_{c.m.}$ [17].

The HF calculations are able to express the kinetic energy density term (τ) and spin-orbit density term ($\overrightarrow{J}$), with the help of extended Thomas-Fermi (ETF) approach. On the basis of semi-classical ETF approximation, the total energy of a nuclear system can be expressed as a function of nucleon density only [24].

1.5 Density Function

The SEDF approach is derived as a function of nucleon density ($\rho(r)$) and its derivatives ($\nabla\rho(r)$). The nucleon density ($\rho(r)$) is represented by different density functions depend-

ing upon the choice of reaction. Some of the most commonly used density functions are the two-parameter Fermi (2pF) density function, its extension three-parameter Fermi (3pF) density and the three-parameter Gaussian (3pG) density model. In the three-parameter density functions i.e. 3pF and 3pG, an additional parameter, the wine-bottle parameter (w) is used in addition to surface thickness (a) and half-density radius (R_0) parameters, which are used in 2pF density function. The wine-bottle parameter (w) influences the tail region, which correspondingly affects the barrier characteristics. Therefore, the barrier characteristics of an ion-ion potential varies with different density functions.

Depending upon the sign of wine-bottle parameter (w), depression or amplification in the central density occurs. In the light mass region, w is negative for 3pF but has a positive value for 3pG density function. But in the heavy mass region, both 3pF and 3pG have positive values of w, for reference see Ref. [8]. It has been observed that 3pF and 3pG density functions show central depression in density for the positive values of w and depression increases as we move from light mass nuclei to the heavy mass nuclei [8, 25]. Further, it has been observed that 2pF density function gives a lower barrier height as compared to the 3pF and 3pG density functions in case of symmetric reactions. The lower barrier height in 2pF comes because of larger R_0 value as compared to three-parameter density functions. So, we can say that 2pF density function fits the fusion data for the symmetric reactions. But in the case of asymmetric reactions, 3pF and 3pG density functions are found to address the experimental data more accurately as compared to 2pF density function, because of the lower barrier height due to larger R_0 value [8].

1.6 Proposed Work

In the present work, some mass-asymmetric reactions forming compound nuclei of mass range $86 \leq A_{CN} \leq 158$ are being considered. To study the corresponding effects in terms of barrier characteristics (V_B, R_B, $\hbar\omega_B$), the 3pF density function is used within the SEDF approach. The above analysis is exercised by employing four different Skyrme forces, i.e., SkTI, MSL0, GSkI and SSk. By considering these forces, one can observe a significant change on barrier characteristics as well as fusion cross-sections, which are calculated by using the well-known Wong formula [26] and its extended version i.e. ℓ-summed Wong formula [27].

So, it would be interesting to see the impact of chosen Skyrme forces in view of chosen set of asymmetric nuclear reactions (^{28,30}Si, ^{36}S, ^{40}Ca, ^{48}Ti+^{58}Ni, and ^{58}Ni+^{90}Zr, ^{92}Mo, ^{94}Zr and ^{100}Mo) with three-parameter Fermi density function within the SEDF approach across the Coulomb barrier energies.

Bibliography

[1] J. J. Thomson, Philos. Mag. **44**, 293 (1897).

[2] E. Rutherford, Phil. Mag. Series 6, vol. **21**, 669-688 (1911).

[3] J. Chadwick, Proc. R. Soc. Lond. A **136**, 692-708 (1932).

[4] R. Planeta, Inter. Jour. of Modern Phys. E Vol. **15**, 973–1068 (2006).

[5] B. V. Jacak, Fragment Production in Intermediate Energy Heavy-Ion Reactions (1984).

[6] I. Dutt and R. K. Puri, Phys. Rev. C **81**, 064609 (2010); **81**, 044615 (2010).

[7] D. Jain, R. Kumar, M. K. Sharma, Nucl. Phys. A **915**, 106–124 (2013).

[8] S. Jain, M. K. Sharma, and R. Kumar, Nucl. Phys. A **997**, 121699 (2020).

[9] K. A. Brueckner *et al*, Phys. Rev. C **173**, 944 (1968).

[10] M. Beiner, R. J. Lombard, Ann. of Phys. **86**, 262-305 (1974).

[11] D. Vautherin, D. M. Brink, Phys. Rev. C **5**, 626 (1972).

[12] K. A. Brueckner, J. L. Gammel, H. Weitzner, Phys. Rev. C **110**, 431 (1958).

[13] Y. J. Nemeth, D. Vautherin, Phys. Lett. **32**B, 561 (1970).

[14] J. W. Negele, Phys. Rev. C **1**, 1260 (1970).

[15] T. H. R. Skyrme, Phil. Mag. **1**, 1043 (1956).

[16] T. H. R. Skyrme, Nucl. Phys. **9**, 615-634 (1959).

[17] M. Dutra *et al*, Phys. Rev. C **85**, 035201 (2012).

[18] Niyti *et al*, Phys. Rev. C **95**, 034602 (2017).

[19] Z. W. Zuo *et al*, Chinese Phys. C **42**, 064106 (2018).

[20] Q. Z. Chai *et al*, Phys. Rev. C **102**, 014312 (2020).

[21] F. Tondeur, Nucl. Phys. A **420**, 297-319 (1984).

[22] L. W. Chen *et al*, Phys. Rev. C **82**, 024321 (2010).

[23] B. K. Agrawal, S. K. Dhiman, R. Kumar, Phys. Rev. C **73**, 034319 (2006).

[24] B. Grammoticos, A. Voros, Ann. Phys. **123**, 359 (1979).

[25] I. Sick, Nucl. Phys. A **218**, 509–541 (1974).

[26] C. Y. Wong, Phys. Rev. Lett. **31**, 766 (1974).

[27] R. Kumar *et al*, Phys. Rev. C **80**, 034618 (2009).

Chapter 2

Methodology

2.1 Skyrme Energy Density Formalism (SEDF)

The total interaction potential is a combination of repulsive and attractive potentials i.e., repulsive Coulomb and centrifugal potential and attractive nuclear potential. It is represented as:

$$V_T(R) = V_C(R) + V_\ell(R) + V_N(R) \tag{2.1}$$

Where $V_C(R)$ represents the repulsive long-range Coulomb potential, $V_\ell(R)$ represents the centrifugal potential and $V_N(R)$ is short-ranged attractive nuclear potential.
The repulsive Coulomb potential between two spherical nuclei having atomic numbers Z_1 and Z_2 can be written as:

$$V_C(R) = \frac{Z_1 Z_2 e^2}{R} \tag{2.2}$$

and the centrifugal potential is given by:

$$V_\ell(R) = \frac{\hbar^2 \ell(\ell+1)}{2\mu R^2} \tag{2.3}$$

Now, the SEDF approach defines the short-range nuclear potential in terms of the expectation values of energy [1, 2], as given below:

$$V_N(R) = E(R) - E(\infty) \tag{2.4}$$

where $E(R)$ is the value of expectation energy when the nuclei are separated by a finite distance R of few fermi (10^{-15}) scale. One can write the expectation energy in terms of an energy density Hamiltonian function $H(R)$ as suggested by Vautherin and Brink [2], as:

$$E(R) = \int H(\overrightarrow{r}) d\overrightarrow{r} \tag{2.5}$$

Similarly, $E(\infty)$ is the value of expectation energy when the nuclei are infinitely separated from each other and can be written as:

$$E(\infty) = \int H_1(\overrightarrow{r})d\overrightarrow{r} + \int H_2(\overrightarrow{r})d\overrightarrow{r} \tag{2.6}$$

The energy density functional is written as [3]:

$$\begin{aligned} H(\rho,\tau,\overrightarrow{J}) = & \frac{\hbar^2}{2m}\tau + \frac{1}{2}t_0\left[\left(1+\frac{1}{2}x_0\right)\rho^2 - \left(x_0+\frac{1}{2}\right)(\rho_n^2+\rho_p^2)\right] \\ & + \frac{1}{12}t_3\rho^\alpha\left[\left(1+\frac{1}{2}x_3\right)\rho^2 - \left(x_3+\frac{1}{2}\right)(\rho_n^2+\rho_p^2)\right] \\ & + \frac{1}{4}\left[t_1\left(1+\frac{1}{2}x_1\right) + t_2\left(1+\frac{1}{2}x_2\right)\right]\rho\tau \\ & - \frac{1}{4}\left[t_1\left(x_1+\frac{1}{2}\right) - t_2\left(x_2+\frac{1}{2}\right)\right](\rho_n\tau_n+\rho_p\tau_p) \\ & + \frac{1}{16}\left[3t_1\left(1+\frac{1}{2}x_1\right) - t_2\left(1+\frac{1}{2}x_2\right)\right](\overrightarrow{\nabla}\rho)^2 \\ & - \frac{1}{16}\left[3t_1\left(x_1+\frac{1}{2}\right) + t_2\left(x_2+\frac{1}{2}\right)\right][(\overrightarrow{\nabla}\rho_n)^2 + (\overrightarrow{\nabla}\rho_p)^2] \\ & - \frac{1}{2}W_0[\rho\overrightarrow{\nabla}.\overrightarrow{J} + \rho_n\overrightarrow{\nabla}.\overrightarrow{J_n} + \rho_p\overrightarrow{\nabla}.\overrightarrow{J_p}]. \end{aligned} \tag{2.7}$$

In the above expression, 'x_i, t_i, W_0 and α' are the parameters of Skyrme interaction. m is the individual nucleon mass, and $\tau = \tau_n + \tau_p$, $\rho = \rho_n + \rho_p$, and $\overrightarrow{J} = \overrightarrow{J_n} + \overrightarrow{J_p}$ are the kinetic energy density, nuclear density and spin-orbit density, respectively. The above discussed Hamiltonian is for old Skyrme interactions, such as SkTI. On the other hand, for MSL0, an additional tensor coupling with spin gradient term is introduced [4]. The Hamiltonian has been adjusted [5] by replacing the third term with

$$\frac{1}{2}\sum_{i=1}^{3} t_{3i}\rho^{\alpha_i}\left[\left(1+\frac{1}{2}x_{3i}\right)\rho^2 - \left(x_{3i}+\frac{1}{2}\right)(\rho_n^2+\rho_p^2)\right] \tag{2.8}$$

and adding a new term due to spin gradient tensor coupling i.e.,

$$-\frac{1}{16}(t_1x_1+t_2x_2)\overrightarrow{J^2} + \frac{1}{16}(t_1-t_2)(\overrightarrow{J_p^2}+\overrightarrow{J_n^2}) \tag{2.9}$$

to obtain new Skyrme forces, GSkI and SSk.

The Kinetic energy density term (taken up to second order) is written by using the

extended Thomas-Fermi model [6], as

$$\tau_q(\overrightarrow{r}) = \frac{3}{5}(3\pi^2)^{2/3}\rho_q^{5/3} + \frac{1}{36}\frac{(\overrightarrow{\nabla}\rho_q)^2}{\rho_q} + \frac{1}{3}\Delta\rho_q + \frac{1}{6}\frac{\overrightarrow{\nabla}\rho_q.\overrightarrow{\nabla}f_q + \rho_q\Delta f_q}{f_q} - \frac{1}{12}\rho_q\left(\frac{\overrightarrow{\nabla}f_q}{f_q}\right)^2 + \frac{1}{2}\rho_q\left(\frac{2m}{\hbar^2}\right)^2\left(\frac{W_0}{2}\frac{\overrightarrow{\nabla}(\rho+\rho_q)}{f_q}\right)^2 \tag{2.10}$$

where f_q is the effective mass form factor, the details can be seen in [3].
The spin-obit density, $\overrightarrow{J}$ using ETF model can be written as:

$$\overrightarrow{J_q}(\overrightarrow{r}) = -\frac{2m}{\hbar^2}\frac{1}{2}W_0\frac{1}{f_q}\rho_q\overrightarrow{\nabla}(\rho+\rho_q) \tag{2.11}$$

i.e., spin-orbit density is also a function of ρ_q and/or ρ only.
For a composite system,

$$\rho = \rho_1 + \rho_2 \tag{2.12}$$

For frozen density approximation,

$$\begin{aligned}\tau(\rho) &= \tau_1(\rho_1) + \tau_2(\rho_2)\\ \overrightarrow{J}(\rho) &= \overrightarrow{J_1}(\rho_1) + \overrightarrow{J_2}(\rho_2)\end{aligned} \tag{2.13}$$

where $\rho_i = \rho_{in} + \rho_{ip}$, $\tau_i(\rho_i) = \tau_{in}(\rho_{in}) + \tau_{ip}(\rho_{ip})$ and $\overrightarrow{J_i}(\rho_i) = \overrightarrow{J_{in}}(\rho_{in}) + \overrightarrow{J_{ip}}(\rho_{ip})$.

2.2 Density Function

In the present work, the nuclear density is calculated by using the two-parameter Fermi (2pF) and three-parater Fermi (3pF) density function.

2.2.1 Two-parameter Fermi (2pF)

The 2pF density function is written as:

$$\rho_i(z_i) = \rho_{0i}\left[1 + exp\left(\frac{z_i - R_{0i}}{a_i}\right)\right]^{-1} \qquad , -\infty \leq z \leq \infty \tag{2.14}$$

Here $i = 1, 2$ represents the projectile and target, resp. and ρ_{0i} is the central density term, which can be calculated by using the nuclear density integral [7],

$$4\pi \int_0^\infty \rho(z) z^2 dz = 1 \tag{2.15}$$

The central density term is written as

$$\rho_{0i} = \frac{3A_i}{4\pi R_{oi}^3} \left[1 + \frac{\pi^2 a_i^2}{R_{0i}^2}\right]^{-1} \tag{2.16}$$

The parameters of 2pF density function i.e., half-density radius (R_{0i}) and surface thickness (a_i) have values in accordance with ref. [8, 9] for the mass region $4 \leq A \leq 238$. Their polynomials are referred from [10] and are acquired by fitting the experimental data [8, 9].

2.2.2 Three-parameter Fermi (3pF)

The 3pF density function [8] is given by:

$$\rho_i(z_i) = \rho_{0i} \left(1 + \frac{w_i z_i^2}{R_{0i}^2}\right) \left[1 + exp\left(\frac{z_i - R_{0i}}{a_i}\right)\right]^{-1} \tag{2.17}$$

Here, ρ_{0i} is the central density term, which is normalized using the integral in Eq. (2.15) and is obtained by following the method in [11],

$$\rho_{0i} = \frac{3A_i}{4\pi R_{0i}^3} \left[1 + \frac{3w_i}{5} + (1 + 2w_i)\frac{\pi^2 a_i^2}{R_{0i}^2} + \frac{7}{5} w_i \frac{\pi^4 a_i^4}{R_{0i}^4}\right]^{-1} \tag{2.18}$$

The parameters of 3pF density function i.e., half-density radius (R_{0i}), thickness (a_i) and wine-bottle parameter (w_i) have values in accordance with ref. [8] for the mass region $14 \leq A \leq 166$, and their polynomials are acquired by fitting the experimental data, as

$$\begin{aligned}
R_{0i} &= 1.56652 + 0.07285A_i - 5.3503 \times 10^{-4} A_i^2 + 1.74857 \times 10^{-6} A_i^3 - 1.23798 \times 10^{-9} A_i^4, \\
a_i &= 0.33614 + 0.01938A_i - 4.79946 \times 10^{-4} A_i^2 + 4.25566 \times 10^{-6} A_i^3 - 1.23125 \times 10^{-8} A_i^4, \\
w_i &= 0.05658 - 0.01174A_i + 1.75649 \times 10^{-4} A_i^2 - 8.96765 \times 10^{-7} A_i^3 + 1.7808 \times 10^{-9} A_i^4.
\end{aligned} \tag{2.19}$$

Here, w_i is dimensionless.

2.3 Fusion Cross-section

To calculate the fusion cross-sections, Wong formula [12] and the extended ℓ-summed Wong formula [13] have been used.

2.3.1 Wong formula and extended ℓ-summed Wong model

According to Wong [12], the fusion cross-section for two spherical colliding nuclear partners is given as a function of the center of mass energy ($E_{c.m.}$), as

$$\sigma_{fus}(E_{c.m}) = \frac{\pi\hbar^2}{2\mu E_{c.m.}} \sum_{\ell=0}^{\ell_{max}} (2\ell+1) T_\ell(E_{c.m.}) \tag{2.20}$$

Where, μ represents the reduced mass and $T_\ell(E_{c.m.})$ is the penetration probability for each angular-momentum (ℓ) through the potential barrier $V_T^\ell(R, E_{c.m.})$, which can be obtained by using the Hill-Wheeler approximation [14, 15], as:

$$T_\ell(E_{c.m.}) = \left[1 + exp\left(\frac{2\pi(V_B^\ell - E_{c.m.})}{\hbar\omega_B^\ell}\right)\right]^{-1} \tag{2.21}$$

Where, V_B^ℓ is the barrier height and $\hbar\omega_B^\ell$ is evaluated at the barrier position $R = R_B^\ell$ corresponding to maximum V_B^ℓ, as

$$\hbar\omega_\ell(E_{c.m.}) = \hbar[|d^2V_T^\ell(R)/dR^2|_{R=R_B^\ell}/\mu]^{1/2}, \tag{2.22}$$

and, the R_B^ℓ is attained from the condition,

$$|dV_T^\ell(R)/dR|_{R=R_B^\ell} = 0 \tag{2.23}$$

Instead of taking ℓ-dependent potentials $V_T^\ell(R, E_{c.m.})$ into consideration and solving the Eq. (2.20) explicitly, Wong [12] executed the summation under particular conditions:

i $\hbar\omega_B^\ell \approx \hbar\omega_B^0$, and

ii $V_B^\ell \approx V_B^0 + \frac{\hbar^2\ell(\ell+1)}{2\mu {R_B^0}^2}$

which means $R_B^\ell \approx R_B^0$ also. That is to say, both V_B^ℓ and $\hbar\omega_\ell$ are obtained for $\ell = 0$. By employing the above approximations, and using an integral instead of ℓ-summation

in Eq. (2.20), Wong yields the formula for $\ell = 0$, as

$$\sigma(E_{c.m.}) = \frac{R_B^{0\,2}\hbar\omega_0}{2E_{c.m.}} ln\left[1 + exp\left(\frac{2\pi}{\hbar\omega_0}(E_{c.m.} - V_B^0)\right)\right] \tag{2.24}$$

Later on, Gupta and collaborators [13] observed that angular-momentum (ℓ) plays an important role while calculating the barrier characteristics and fusion cross-section. Therefore, the ℓ-summation is carried out explicitly in the Eq. (2.20). One may put an upper limit to the ℓ-values to avoid the overestimation of fusion cross-sections over the experimental data.

Bibliography

[1] K. A. Brueckner *et al*, Phys. Rev. C **173**, 944 (1968).

[2] D. Vautherin, D. M. Brink, Phys. Rev. C **5**, 626 (1972).

[3] R. Kumar, M. K. Sharma, R. K. Gupta, Nucl. Phys. A **870-871**, 42-57 (2011).

[4] L. W. Chen *et al*, Phys. Rev. C **82**, 024321 (2010).

[5] B. K. Agrawal, S. K. Dhiman, R. Kumar, Phys. Rev. C **73**, 034319 (2006).

[6] J. Bartel, K. Bencheikh, Eur. Phys. J. A **14**, 179 (2002).

[7] L. R. B. Elton, Nuclear Sizes, Oxford University Press, London (1961).

[8] H. D. Vries *et al*, At. Data Nucl. Data Tables **36**, 495–536 (1987).

[9] L. R. B. Elton, Proc. Phys. Soc. Lond. A **63**, 1115 (1950).

[10] R. K. Gupta *et al*, Phys. Rev. C **75**, 024603 (2007).

[11] L. Zhang *et al*, Mod. Phys. Lett. A **32** (36), 1750195 (2017).

[12] C. Y. Wong, Phys. Rev. Lett. **31**, 766 (1974).

[13] R. Kumar *et al*, Phys. Rev. C **80**, 034618 (2009).

[14] D. L. Hill and J. A. Wheeler, Phys. Rev. **89**, 1102 (1953).

[15] T. D. Thomas, Phys. Rev. **116**, 703 (1959).

Chapter 3

Fusion dynamics of mass-asymmetric reactions using Skyrme based nuclear potentials

3.1 Results and discussions

The Skyrme Energy Density Formalism (SEDF), can be employed to estimate the nuclear potential in terms of various density parameters, which in turn helps to comprehend the heavy-ion induced reaction dynamics. In a recent work, the authors of Ref. [1] have investigated the influence of two-parameter Fermi (2pF), three-parameter Fermi (3pF) and three-parameter Gaussian (3pG) density functions in terms of barrier characteristics and subsequently in reference to fusion cross-sections of ^{58}Ni-based mass-symmetric ($\eta_A = \frac{|A_1-A_2|}{A_1+A_2}$=0) and mass-asymmetric ($\eta_A \neq 0$) reactions. As a result, the use of two-parameter Fermi density function within SEDF is found to address the experimental data related to the symmetric reaction (^{58}Ni+^{58}Ni), whereas, the three-parameter density function seems to provide a better choice for addressing the below barrier anomalies of mass-asymmetric reactions, i.e. ^{8}B, ^{18}O and ^{132}Sn+^{58}Ni.

In the present work, the main intention is to have a further insight into the fusion dynamics of mass-asymmetric nuclear reactions (^{28,30}Si, ^{36}S, ^{40}Ca, ^{48}Ti, ^{90,94}Zr and ^{92,100}Mo+^{58}Ni), at the low-energy regime. The projectile nuclei of varying mass, ranging from $A_1 = 28 - 100$ are striked on common target ^{58}Ni, in the chosen set of asymmetric reactions. For this analysis, different sets of Skyrme force parameters (SkTI, MSL0, GSkI and SSk) are used in the framework of three-parameter Fermi (3pF) density function to study the corresponding effects on the barrier characteristics. Further, to observe the collective effects of fusion barrier parameters, the fusion cross-sections (σ_{fus}) are calculated by employing the Wong formula [2] and its extension i.e. ℓ-summed Wong model [3], across the Coulomb barrier energies. The calculated fusion cross-sections are compared with the available experimental data [4]-[9] of considered choice of mass-asymmetric nuclear fusion reactions.

3.1.1 Comparison of Two-parameter and Three-parameter Fermi density functions in terms of total interaction potential

Initially, for comparison, the total interaction potential V_T (MeV) has been plotted using the two-parameter Fermi (2pF) and three-parameter Fermi (3pF) density functions, as shown in Fig.3.1 (a) for mass-symmetric (^{58}Ni+^{58}Ni) and (b) mass-asymmetric

(^{28}Si+^{58}Ni) reactions. Also, the behavior of projectile's density obtained due to 2pF and 3pF density functions is analyzed as a function of nuclear radius, see the lower panels (c) and (d) of Fig.3.1. Since, the target (^{58}Ni) is fixed in the above mentioned reactions. One can see from Fig.3.1 for ^{58}Ni+^{58}Ni (symmetric) reaction that, the 3pF density function gives relatively higher barrier height (V_B) from that of two-parameter density function. However, for mass-asymmetric colliding nuclear partners (^{28}Si+^{58}Ni), V_B obtained using 3pF density function becomes lower w.r.t. 2pF density function.

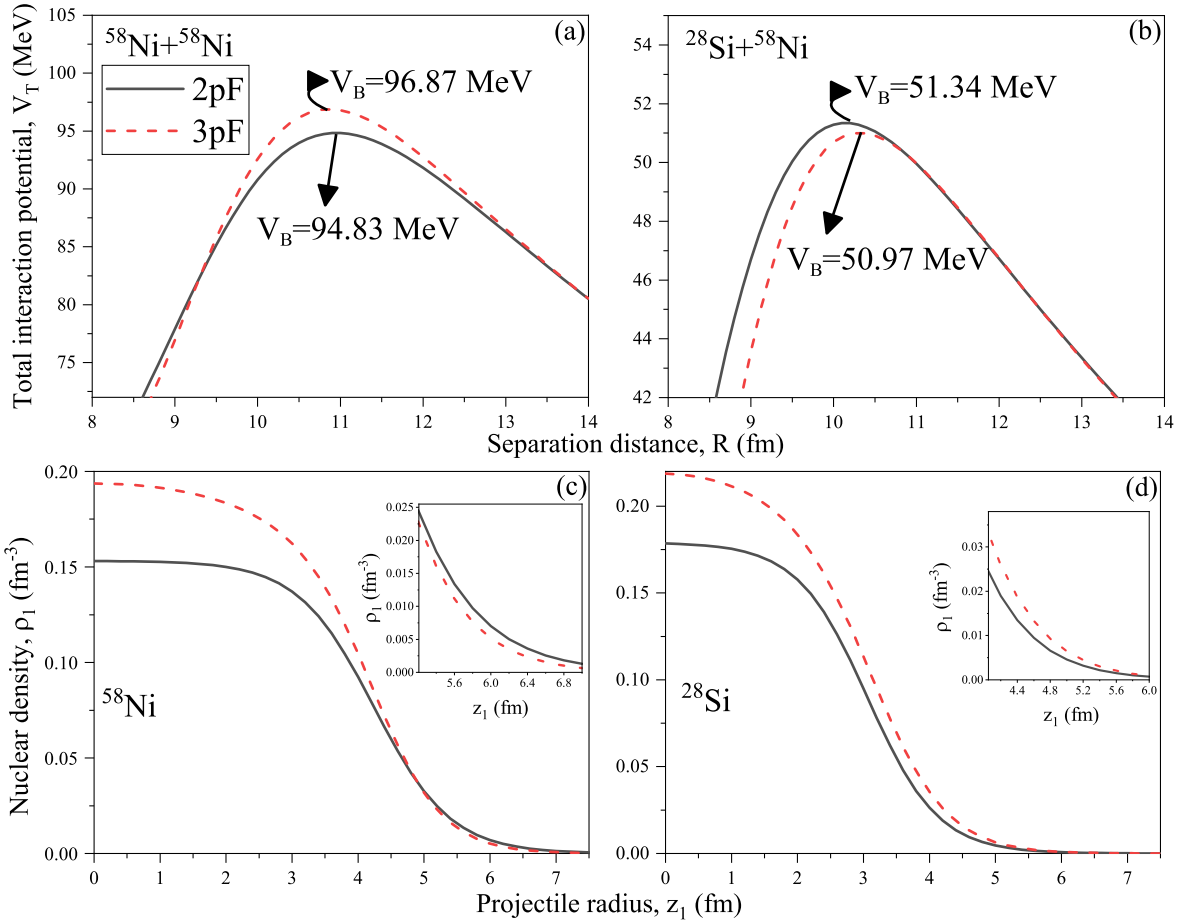

Figure 3.1: The variation of total interaction potential V_T(MeV), obtained due to two- (2pF) and three-parameter Fermi (3pF) density functions, w.r.t. the separation distance R (fm) for (a) mass-symmetric (^{58}Ni+^{58}Ni) and (b) asymmetric (^{28}Si+^{58}Ni) nuclear reactions. Additionally, panels (c) and (d) represent the density $\rho_1(fm^{-3})$ profile of projectile of the above mentioned reactions.

In nuclear fusion reactions, the surface interactions play important role between two colliding nuclei, which can be analysed from the tail region of density profile. In view of this, one can see the behavior of projectile's density ρ_1 (fm^{-3}) profile of ^{28}Si and ^{58}Ni+^{58}Ni reactions as a function of nuclear radius z_1 (fm), see panels (c) and (d) of Fig.3.1 respec-

tively. The 3pF density is found to give comparatively smaller value than that of 2pF, in the tail region, for projectile of symmetric reaction (see panel (c) of Fig.3.1). As a consequence, V_B obtained due to 3pF is higher than 2pF density function. On the other hand, in the density profile of ^{28}Si (which is projectile of mass-asymmetric reaction), $\rho_1(fm^{-3})$ obtained due to 3pF show relatively higher value in the tail region than that of 2pF density function, see panel (d), which in turn lowers the barrier height of 3pF density functions. For more clarity, the behavior of ρ_1 in its tail region can be seen in the insets given in the lower panels of Fig.3.1.

On the basis of above analysis, one can say that, the three-parameter Fermi (3pF) density function used within the SEDF approach gives relatively lower barrier and subsequently give larger possibility for the fusion among target-projectile of mass-asymmetric reactions. Thus, further calculations are done using the three parameter Fermi (3pF) density function for a variety of nuclear systems, formed using common target ^{58}Ni and variable mass projectile, ranging from ^{28}Si to ^{100}Mo. The associated analysis is exercised using different Skyrme interactions, i.e. SkTI, MSL0, GSkI and SSk, within the Skyrme Energy Density Formalism (SEDF).

3.1.2 Use of different Skyrme forces in the fusion dynamics of mass-asymmetric reactions

In Fig. 3.2, a comparative analysis of four Skyrme forces i.e. SkTI, MSL0, GSkI and SSk is shown by plotting the total ion-ion interaction potential V_T(MeV) as a function of separation distance R(fm). It is clear from Fig. 3.2 that, Skyrme force SkT1 provides a much higher barrier in comparison to the other Skyrme interactions used. This analysis hold true for all the considered choices of ^{58}Ni-based mass-asymmetric reactions, i.e. ^{28,30}Si, ^{36}S, ^{40}Ca, ^{48}Ti, ^{90,94}Zr and ^{92,100}Mo+^{58}Ni, see panels (a)-(i) of Fig.3.2. From this figure, one can also notice that, the barrier parameters (V_B, R_B and $\hbar\omega_B$) obtained due to MSL0, GSkI and SSk Skyrme forces are almost of similar values. A remarkable difference in V_B of about 2 - 5 MeV is observed between SkTI and the other selected choices of Skyrme forces (MSL0, GSkI and SSk), as one moves from A_{CN}=86 to 158. The corresponding effects can be analyzed further in the calculation of fusion cross-sections, across the Coulomb barrier energies.

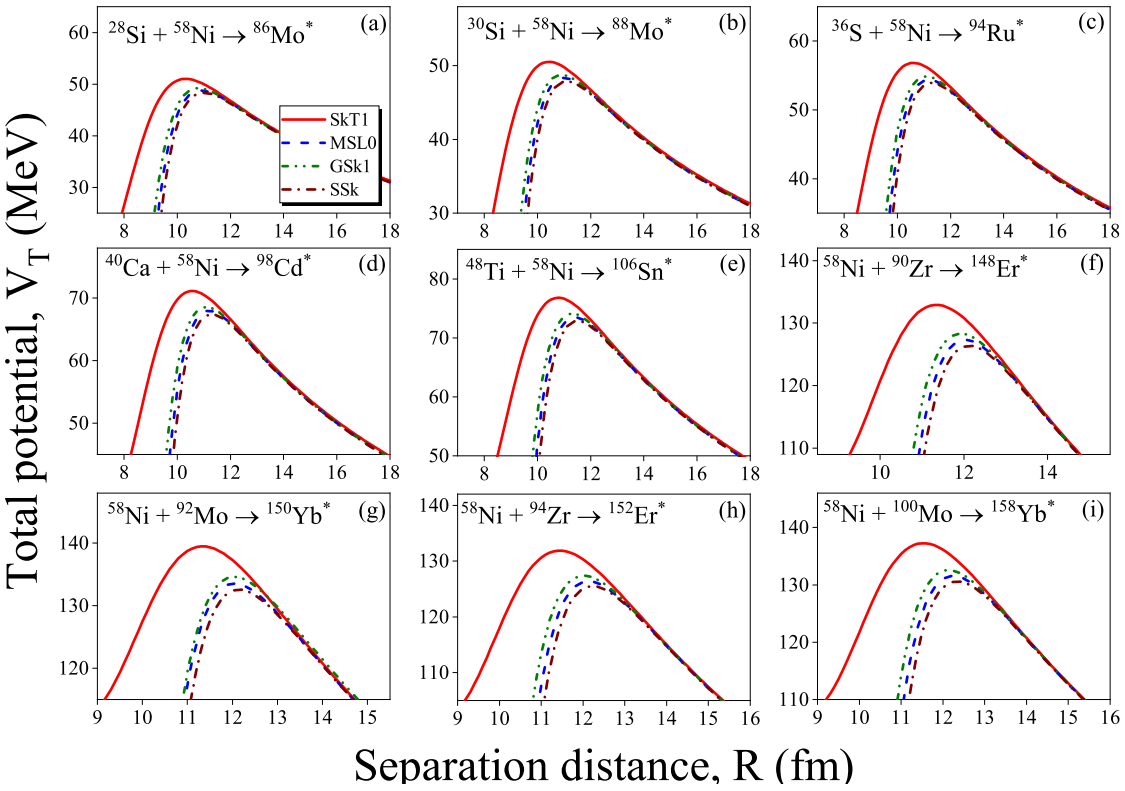

Figure 3.2: The total interaction potential (V_T), for mass-asymmetric nuclear reactions forming the compound nucleus of mass range $86 \leq A_{CN} \leq 158$, is plotted against the separation distance (R) for different Skyrme forces i.e. SkT1, MSL0, GSkI and SSk.

3.1.3 Calculation of Fusion cross-sections for ^{58}Ni-based mass-asymmetric reactions

For the considered choices of mass-asymmetric ($\eta_A \neq 0$) reactions, i.e. ^{28,30}Si, ^{36}S, ^{40}Ca, ^{48}Ti+^{58}Ni, ^{58}Ni+^{90,94}Zr and ^{92,100}Mo, the fusion cross-sections (σ_{fus}) are available at energies near and around the Coulomb barrier [4]-[9]. In view of this, σ_{fus} are calculated using the Wong formula, which depends on the barrier characteristics (V_B, R_B and $\hbar\omega_B$), for the considered nuclear reactions, see Fig.3.3. From this figure, it is noticed that, σ_{fus} obtained using SkTI Skyrme force overestimates the experimental data for ^{28,30}Si and ^{36}S+^{58}Ni reactions and reasonably accounts the data across the barrier energies for ^{40}Ca+^{58}Ni, see panels (a)-(d) of Fig.3.3. For other choices of reactions (^{48}Ti, ^{90,94}Zr and ^{92,100}Mo+^{58}Ni), there is fusion hindrance in σ_{fus} obtained due to SkTI, at the below-barrier energies beside usual overestimation in the above barrier region, see (e)-(i) of Fig.3.3. For SkTI force, the hindrance enhances as one moves towards heaviest mass compound nucleus, formed from above mentioned reaction. Besides this, the calculation of σ_{fus} with the other considered choices of Skyrme forces (MSL0, GSkI and SSk), which

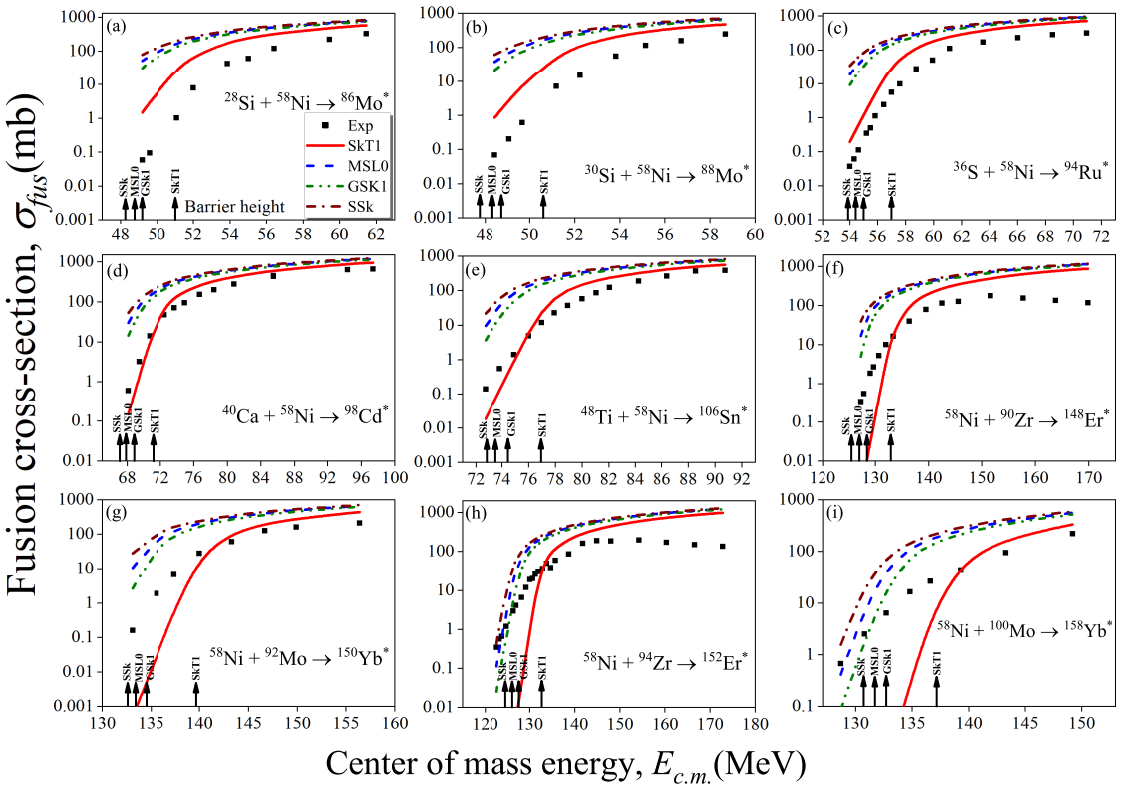

Figure 3.3: Fusion cross-sections calculated using Wong formula [2] for mass-asymmetric reactions forming the compound nucleus of mass range $86 \leq A_{CN} \leq 158$, by using the 3pF density function within the SEDF approach with different Skyrme forces, i.e. SkT1, MSL0, GSkI and SSk. The upward arrows indicate the barrier height, for mentioned Skyrme forces.

give almost similar barrier characteristics, is found to overestimate the experimental data across the Coulomb barrier energies. This result is true for all the selected choices of ^{58}Ni-based mass-asymmetric reactions. However, it is important to mention that, for the last two reactions forming heavy-mass compound nuclei (^{152}Er* and ^{158}Yb*), GSkI and MSL0 show hindrance only at the lowest incident energy $E_{c.m.}$, see panels (h) and (i) of Fig.3.3.

The above observed analysis is based on the barrier height (V_B) obtained due to different sets of Skyrme force parameters (SkTI, MSL0, GSkI and SSk) and their values, for all the considered choices of mass-asymmetric nuclear reactions, are listed in Table 3.1. The highest barrier height of SkTI followed by GSkI, MSL0 and SSk forces impact the fusion cross-sections, accordingly, especially at energies in the below barrier region. In this table, the difference between the lowest incident energy ($E_{c.m.}$) and V_B is also shown, which indicates for which force the lowest incident energy (acquired by the projectiles of above mentioned reactions) belongs to the below-, near- or above-barrier region. For SkTI force,

Table 3.1: The calculated barrier height, V_B for asymmetric nuclear reactions (^{28,30}Si, ^{36}S, ^{40}Ca, ^{48}Ti+^{58}Ni, and ^{58}Ni+^{90}Zr, ^{92}Mo, ^{94}Zr and ^{100}Mo) using different Skyrme forces, within SEDF approach.

Reaction	Barrier height (V_B (MeV))				$E_{c.m.} - V_B$ (MeV)			
	SkTI	GSkI	MSL0	SSk	SkTI	GSkI	MSL0	SSk
^{28}Si+^{58}Ni	51.007	49.194	48.756	48.316	-1.827	-0.014	0.424	0.864
^{30}Si+^{58}Ni	50.517	48.754	48.315	47.896	-2.067	-0.304	0.135	0.554
^{36}S+^{58}Ni	56.828	54.859	54.380	53.921	-2.818	-0.849	-0.370	0.089
^{40}Ca+^{58}Ni	71.118	68.569	67.971	67.395	-3.180	-0.469	0.129	0.705
^{48}Ti+^{58}Ni	76.797	74.106	73.469	72.867	-4.067	-1.376	-0.739	-0.137
^{58}Ni+^{90}Zr	132.900	128.341	127.328	126.409	-5.600	-1.041	-0.028	0.891
^{58}Ni+^{92}Mo	139.474	134.605	133.542	132.569	-6.374	-1.505	-0.442	0.531
^{58}Ni+^{94}Zr	131.855	127.391	126.393	125.494	-9.155	-4.691	-3.693	-2.794
^{58}Ni+^{100}Mo	137.258	132.563	131.535	130.607	-8.558	-3.863	-2.835	-1.907

the difference $E_{c.m.} - V_B$ becomes relatively more negative, with the increase in the mass of compound nuclear system, as compared to other forces. From this difference of $E_{c.m.}$ and V_B, one can simply conclude that the force which gives the highest barrier height would hinder the fusion among two nuclei of mass-asymmetric reactions. On the other hand, for other considered Skyrme forces (GSkI, MSL0 and SSk), the lowest value of $E_{c.m.}$ is either near or above the barrier height. As a consequence, a relatively larger amount of fusion cross-sectional area is obtained due to these forces in the below barrier region, as discussed and shown in Fig.3.3.

As said earlier in Fig.3.3, SkTI shows hindrance at below-barrier region for heavy-mass compound nuclei (CN) and overestimates the data for the lighter-mass CN across the Coulomb barrier energies. Also, σ_{fus} obtained using GSkI, MSL0, and SSk shows overestimation from the data of mass-asymmetric reactions. Because in the Wong formula, σ_{fus} are summed up for infinite values of angular momentum ℓ [2]. In order to overcome the overestimation issue, we have calculated the σ_{fus} by using the extended ℓ-summed Wong formula [3], as shown in Fig.3.4. Here, the maximum value of ℓ is obtained by utilizing the sharp cut-off model [10] for energies in the above barrier region and extended the values for below barrier energies. In results, SkTI force is found to address the data of ^{28,30}Si+^{58}Ni reactions around the Coulomb barrier energies, see panels (a) and (b) respectively of Fig.3.4. However, this force hinders the fusion among target-projectile of other considered mass-asymmetric reactions. On the other hand, GSkI, MSL0 and SSk Skyrme

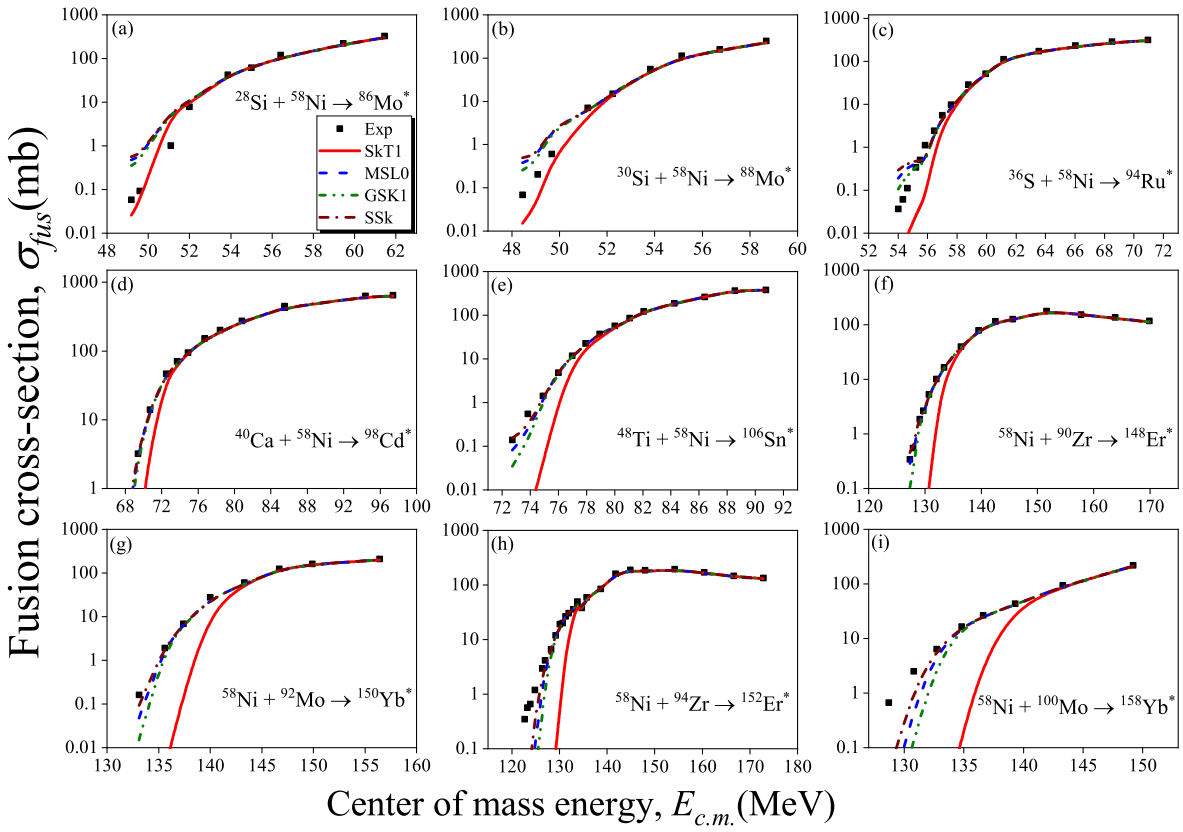

Figure 3.4: Similar to Fig.3.3, but using extended ℓ-summed Wong model [3].

interactions provide comparatively better results particularly at the below-barrier region, see panels (c)-(i) of Fig.3.4. In other words, Skyrme interactions MSL0, GSkI and SSk seem to provide better results at both above and below barrier energies for the chosen set of mass-asymmetric nuclear reactions.

From the above results and related discussions, one may conclude that, SkTI Skyrme force which gives the highest barrier height addresses the fusion data using extended ℓ-summed Wong model for lighter mass compound nuclei formed from ^{28,30}Si+^{58}Ni reactions. However, the other set of Skyrme forces (GSkI, MSL0 and SSk) give better agreement with the data across the Coulomb barrier energies of heavier mass compound nuclei, formed using the rest choices of mass-asymmetric reaction partners.

Summary

In the present work, the main purpose is to study the fusion dynamics of mass-asymmetric reactions (^{28,30}Si, ^{36}S, ^{40}Ca, ^{48}Ti+^{58}Ni, and ^{58}Ni+^{90}Zr, ^{92}Mo, ^{94}Zr and ^{100}Mo) with the use of different sets of Skyrme forces, i.e. SkTI, GSkI, MSL0 and SSk. The three-parameter Fermi (3pF) density function is implemented within the Skyrme Energy Density Formalism (SEDF), since it shows lower barrier height as compared to the two-parameter Fermi (2pF) density function, for the chosen set of mass-asymmetric nuclear partners.

It has been observed in the calculations of fusion cross-sections (σ_{fus}) using ℓ-summed Wong model that, the Skyrme force SkTI which gives the highest barrier height (followed by GSkI, MSL0 and SSk forces) addresses the data for ^{28,30}Si+^{58}Ni reactions, across the Coulomb barrier energies. On the other hand, for other choices of nuclear partners (^{36}S, ^{40}Ca, ^{48}Ti+^{58}Ni, ^{58}Ni+^{90}Zr, ^{92}Mo, ^{94}Zr and ^{100}Mo), GSkI, MSL0 and SSk forces give better results as compared to SkTI force.

Future Scope: In the present work, the target-projectile combinations are assumed to have spherical shape. In the future work, one can extend the idea of exploring the relevance of chosen set of Skyrme forces in the fusion as well as fission dynamics of a wider variety of mass-asymmetric reactions, by including the deformation and orientation effects.

Bibliography

[1] S. Jain, M. K. Sharma, and R. Kumar, Nucl. Phys. A **997**, 121699 (2020).

[2] C Y Wong, Phys. Lett. B **31**, 766 (1973).

[3] R. Kumar *et al*, Phys. Rev. C **80**, 034618 (2009).

[4] A. M. Stefanini *et al*, Phys. Rev. C **30**, 6 (1984).

[5] A. M. Stefanini *et al*, Phys. Lett. **162B**, 66 (1985).

[6] B. Sikora *et al*, Phys. Rev. C **20**, 2219 (1979).

[7] A. M. Vinod Kumar *et al*, Phys. Rev. C **53**, 803 (1996).

[8] F. Scarlassara *et al*, Z. Phys. A - Hadrons and Nuclei **338**, 171-181 (1991).

[9] K. E. Rehm *et al*, Phys. Lett. B **317**, 31-35 (1993).

[10] M. Beckerman *et al*, Phys. Rev. C **23**, 4 (1981).